Accepted Manuscript

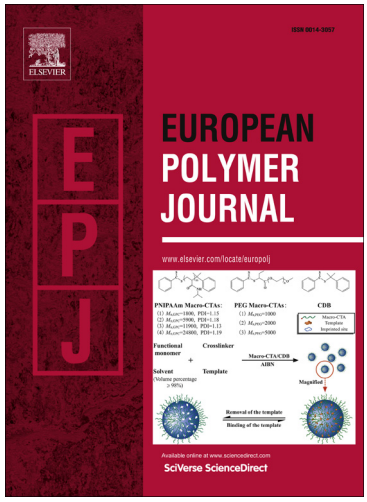

Effect of New Hyperbranched Polyester of Varying Generations on Toughening of Epoxy Resin through Interpenetrating Polymer Networks using Urethane Linkages

D. Manjula Dhevi, S.N. Jaisankar, Madhvesh Pathak

PII: S0014-3057(13)00358-3
DOI: http://dx.doi.org/10.1016/j.eurpolymj.2013.06.041
Reference: EPJ 6173

To appear in: *European Polymer Journal*

Received Date: 20 February 2013
Accepted Date: 17 June 2013

Please cite this article as: Manjula Dhevi, D., Jaisankar, S.N., Pathak, M., Effect of New Hyperbranched Polyester of Varying Generations on Toughening of Epoxy Resin through Interpenetrating Polymer Networks using Urethane Linkages, *European Polymer Journal* (2013), doi: http://dx.doi.org/10.1016/j.eurpolymj.2013.06.041

Effect of New Hyperbranched Polyester of Varying Generations on Toughening of Epoxy Resin through Interpenetrating Polymer Networks using Urethane Linkages

D. Manjula Dhevi[1], S.N. Jaisankar[2], Madhvesh Pathak[1,*]

[1]Centre for Nanomaterials, Department of Chemistry, School of Advanced Sciences, Vellore Institute of Technology University, Vellore 632014, INDIA.

[2]Polymer Lab, Central Leather Research Institute, Adyar, Chennai 600 020, INDIA.

*Correspondence: Dr. Madhvesh Pathak, Department of Chemistry, Vellore Institute of Technology University, Vellore 632014, INDIA. E-mail: madhveshpathak@vit.ac.in

Abstract

In this study, a previously unreported methodology is attempted to improve the inherent brittleness in diglycidyl ether of bisphenol-A based epoxy resin using hyperbranched polymers as toughening agents. Four different hyperbranched polyesters (HBPs) with increasing generations (1 to 4, denoted as HBP-G1 to HBP-G4) were synthesized by reacting calculated amount of dipentaerythritol (used as a core) and dimethylol propionic acid (AB_2 type monomer) through pseudo one-step melt polycondensation method. The newly synthesized HBPs were characterized using spectral, thermal and physical measurements, which confirmed the formation of highly branched structure and decreasing thermal stability with increasing HBP generations. Further, toughening of the epoxy resin is carried out by reacting each generation of the HBP with epoxy using hexamethylene diisocyanate as an intermediate linkage resulting in the formation of HBP-Polyurethane/Epoxy-g-Interpenetrating Polymer Networks (HBP-PU/EP-g-IPNs). A linear polyol-PU/EP-g- IPN is also synthesized for the purpose of comparison. It is found that the HBP modified epoxy samples exhibited higher toughness in comparison to that of neat epoxy and linear polyol based epoxy samples. On the other hand, flexural properties, thermal stability and glass transition temperature of the modified samples is lower than neat epoxy sample due to the existence of flexible urethane linkages and decrease in the cross-linking density of epoxy matrix. The toughening characteristics exhibited by the HBPs are corroborated from the existence of heterogeneous morphology using SEM data.

Keywords: Hyperbranched polyesters; epoxy resin; polyurethane; graft interpenetrating polymer networks; thermal properties; impact behavior.

1. Introduction

Epoxy resins are well-known to exhibit excellent mechanical, thermal and electrical properties, good dimensional stability, and resistance to moisture, corrosion and chemicals. However, the effective usage of cured epoxy resin as structural composites is restricted due to its poor impact resistance which is associated with high brittleness caused by heavily cross-linked structures [1]. This problem has been solved either by reducing the crosslink density of the epoxy network or by toughening the epoxy resin using secondary components such as low molecular weight rubbers [2,3], functionally terminated engineering thermoplastics [4-6], rigid phase [7], interpenetrating polymer networks [8-12], etc. However, they can affect the processing ability of epoxy resin by an undesired increase in its viscosity. This problem can be overcome by adding secondary components such as hyperbranched polymers.

Hyperbranched polymers possess lower viscosity than linear polymers with the same molar mass, are soluble in most of the organic solvents, their end groups can be tailored, and can be employed as a modifier that can simultaneously act as toughening agents. Boogh and his coworkers employed hyperbranched polymer as a toughener for epoxy resins in 1999 [13]. Hydroxyl-terminated [14] and epoxy-terminated [15] hyperbranched polymers were used to toughen the epoxy resin as a function of varying weight content of the toughening agent. Only few researchers have studied the effect of varying generations and different molecular weight of hyperbranched polymers, and have invariably reported an increase in toughening performance with respect to the neat epoxy resin [16, 17]. Among the varying content of epoxy terminated hyperbranched polyester used to enhance the interlaminar toughness of carbon/epoxy composites, 7.5 wt.-% of its content was reported as the best compromise between a slight loss in stiffness and a gain of 60 % in fracture toughness [18].

Apart from hyperbranched polymers, many research groups [19-25] have also dealt with the toughening of epoxy resin using polyurethane (PU) as a modifier via interpenetrating polymer network grafting (g-IPN) methodology. Frisch et al were the pioneer in investigating the properties of PU/Epoxy-g-IPNs [19]. Wang and Chen [20] reported an effective increase in toughness of epoxy resin using hydroxyl terminated PU compared to amine terminated PU. Harani et al [21] incorporated Desmophen 1200-based PU prepolymer as a modifier at different concentrations with the epoxy resin via chemical grafting method, but observed insignificant increase in the mechanical properties. In another report, the addition of 15 wt.-% caprolactam

blocked methylenediphenyl diisocyanate (CMDI) into the epoxy improved the impact strength to an appreciable extent with respect to unmodified epoxy system, which was attributed to the influence of long molecular chain with flexible group (-NH-CO-) present in CMDI skeleton. In the same study, the addition of bismaleimide into both epoxy and CMDI toughened epoxy resin reduced the impact strength [22].

Even though plethora of articles are reported regarding the toughening of epoxy resins using various modifiers and methods, in the present study, we have attempted a novel method for toughening of epoxy resin by chemical blending through the formation of graft interpenetrating polymer networks (graft-IPNs) using HBP as a modifier. In this work, the synthesis of an previously unreported dipentaerythritol (DIPE) based hyperbranched polyester (HBP) as a function of different generations (HBP-G1 to HBP-G4) by pseudo one-step melt polycondensation method are carried out. By following a new methodology, the synthesized HBPs were chemically blended with epoxy resin by using hexamethylene diisocyanate as a reactive intermediate, resulting in urethane linkages between HBP and epoxy resin. The performance of the HBP-PU/EP-g-IPNs having branched structure was correlated with unmodified cured epoxy resin possessing highly cross linked structure as well as a polyol based PU/EP sample having linear structure. The synthesis, characterization and analysis of the IPNs are reported in detail here.

2. Experimental

2.1. Materials

Dipentaerythritol (DIPE), dimethylol propionic acid (DMPA), *p*-toluenesulphonic acid (*p*-TSA), hexamethylene diisocyanate (HMDI), polyethylene glycol of 600 (PEG-600), dibutyltin dilaurate (DBTDL), anhydrous $CHCl_3$ and DMF were purchased from Aldrich, Korea. Epoxy resin (diglycidyl ether of bisphenol-A type, YD-115, epoxide eq. wt. of 180-194) and the curing agent (Polyamidoamine, G-A0533) were obtained from Kukdo Chemicals, Korea. All the above chemicals were used as received.

2.2. Synthesis of HBP polyols by pseudo one-step method

HBP polyol of generations 1 to 4 (HBP-G1 to HBP-G4) were synthesized separately by pseudo one-step method which can be termed as the sequential addition of a monomer with each addition corresponding to the stoichiometric amount for the next theoretical generation by melt polycondensation technique [26]. The synthesis of HBP-G1 is given as follows: 1 mole of DIPE (used as a core) is reacted with 6 moles of DMPA (used as AB_2 type monomer) and *p*-TSA (0.05 wt.-% of DMPA) in a three-necked flat-bottomed flask equipped with a nitrogen inlet, guard tube, mechanical stirrer and placed in an oil bath. After raising the temperature slowly from room temperature to 165 ^{o}C, the reaction was continued at 165 ^{o}C for about 22 h to complete the esterification reaction. Further reaction was carried out under reduced pressure for about 1 h to remove water (formed as a by-product) and also to increase the molecular weight of HBP-G1. The aforementioned procedure is adopted for synthesizing HBP-G2 (28 h), HBP-G3 (33 h), and HBP-G4 (42 h). Molar ratios of the reactants used in the synthesis of HBP-1 to HBP-4 and their reaction pathway are given in Table 1 and in Schemes 1 to 4, respectively.

Table 1

Molar ratios used for synthesizing for different generations of HBPs.

HBPs generation	DIPE (mole)	DMPA (mole)
G1	1	6
G2	1	18
G3	1	42
G4	1	90

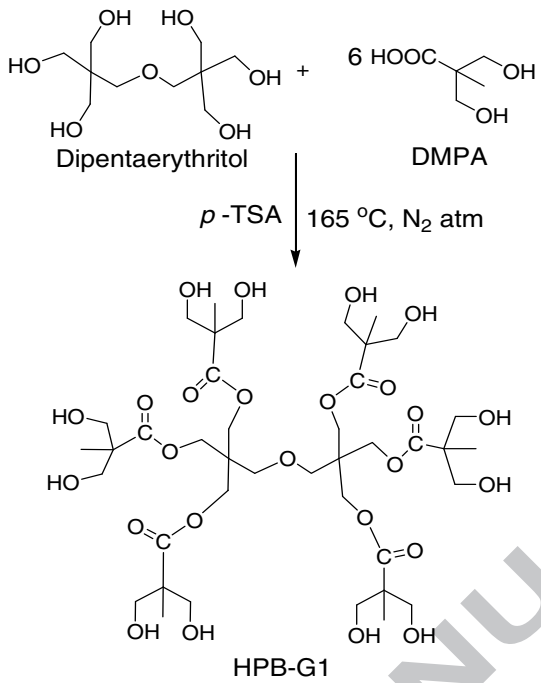

Scheme 1 Synthesis of HBP-G1 showing its idealized structure.

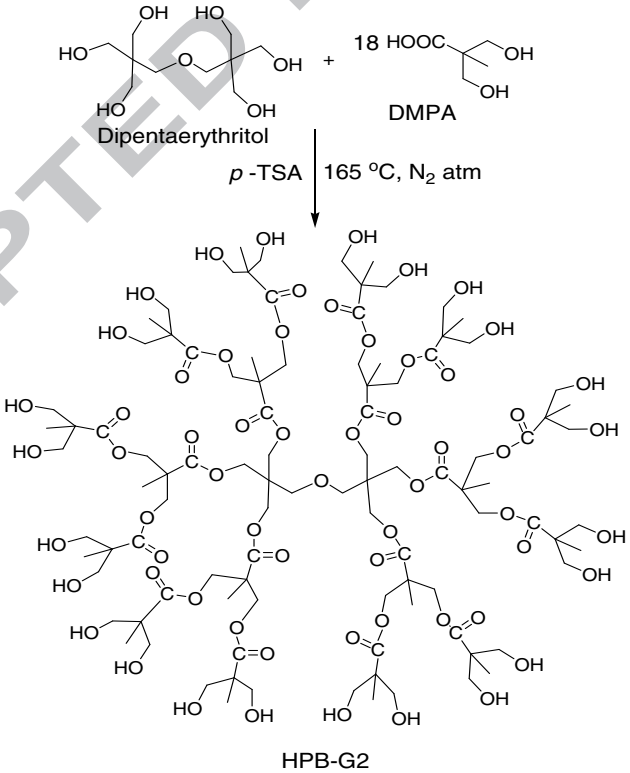

Scheme 2 Synthesis of HBP-G2 showing its idealized structure.

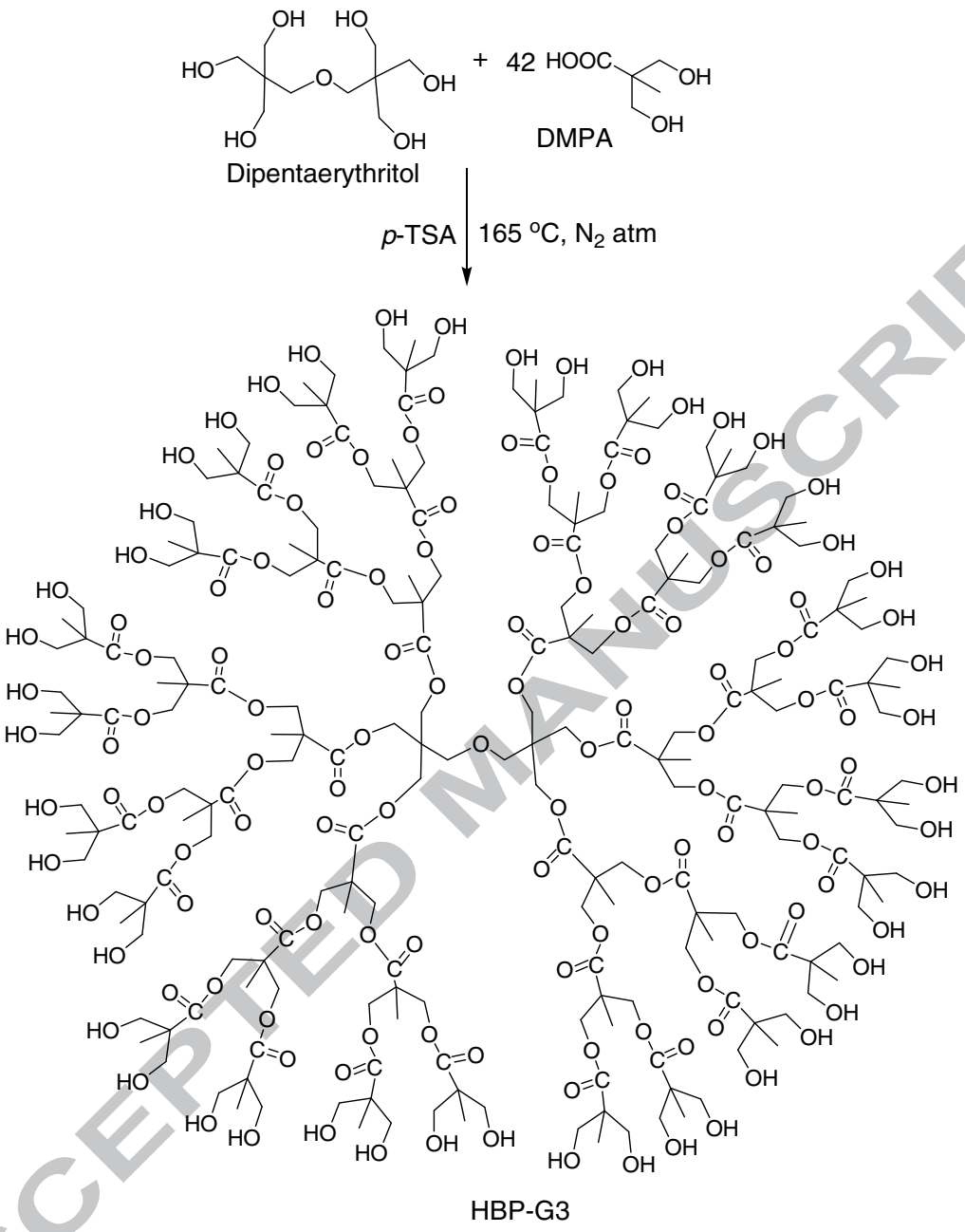

Scheme 3 Synthesis of HBP-G3 showing its idealized structure.

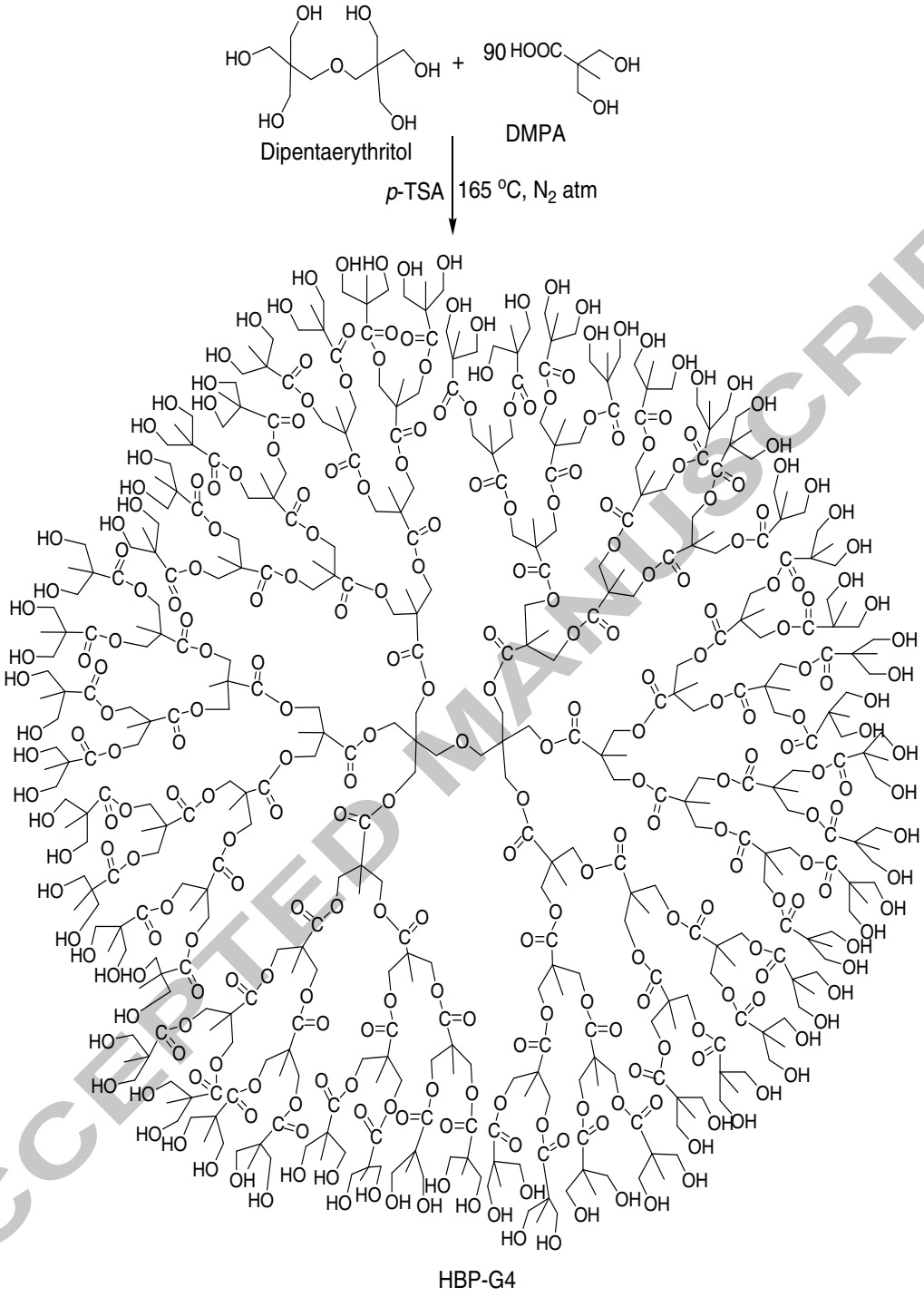

Scheme 4 Synthesis of HBP-G4 showing its idealized structure.

2.3. Synthesis and curing of HBP-PU/Epoxy-g-IPNs

Calculated amount of epoxy resin and HBP-G1 were added to 5 ml of anhydrous DMF solvent in a 250 ml round-bottomed flask equipped with nitrogen inlet, mechanical stirrer, guard tube, and placed in an oil bath. A homogenous solution was obtained after stirring at 120 ^{o}C for 1.5 h, and further stirring was continued at 80 ^{o}C under reduced pressure to remove moisture, if any. To this reaction mixture, calculated amount of HMDI and DBTDL in anhydrous $CHCl_3$ solvent was added drop-wise for about 0.5 h at 90 ^{o}C under reflux setup and a constant flow of nitrogen with vigorous stirring. The reaction was continued for 3 h, and the final product is cooled to room temperature. Calculated amount of curative was added to the above mixture under continuous stirring, then poured into a preheated Teflon mold and kept in a vacuum oven at 80 ^{o}C for 15 min to remove the entrapped air. Curing and post-curing of HBP(G1)-PU/EP samples was carried at 80 ^{o}C for 14 h and at 120 ^{o}C for 2 h, respectively. The aforementioned procedure was adopted in the case of HBP-G2, HBP-G3, HBP-G4 and linear polyol (LP). Composition of the reactants used for preparing the sheets is given in Table 2 and the reaction pathway in Scheme 5. The NCO/OH ratio is maintained at 2 and the amount of HBP-PU in epoxy is maintained at 10 wt.-% irrespective of the generations used and the same weight percentage is used for L-PU sample. The control sample (neat epoxy) was mixed with the curative (50 wt.-% of epoxy) and curing was carried out at 80 ^{o}C for 14 h and post-curing at 120 ^{o}C for 2 h. Epoxy resin was subjected to vacuum for 2 h at 80 ^{o}C prior to synthesis.

Table 2

Amount of reactants (g) used for synthesizing PU/Epoxy-g-IPNs.

Sample Code	Epoxy	Linear Polyol	HBP polyol	HMDI	DBTDL	Curative
Epoxy	100	-	-	-	-	50
L-PU/EP	90	6.4075	-	3.5925	0.05	45
G1-PU/EP	90	-	7.3870	2.6130	0.05	45
G2-PU/EP	90	-	8.7450	1.2550	0.05	45
G3-PU/EP	90	-	9.3847	0.6153	0.05	45
G4-PU/EP	90	-	9.6953	0.3047	0.05	45

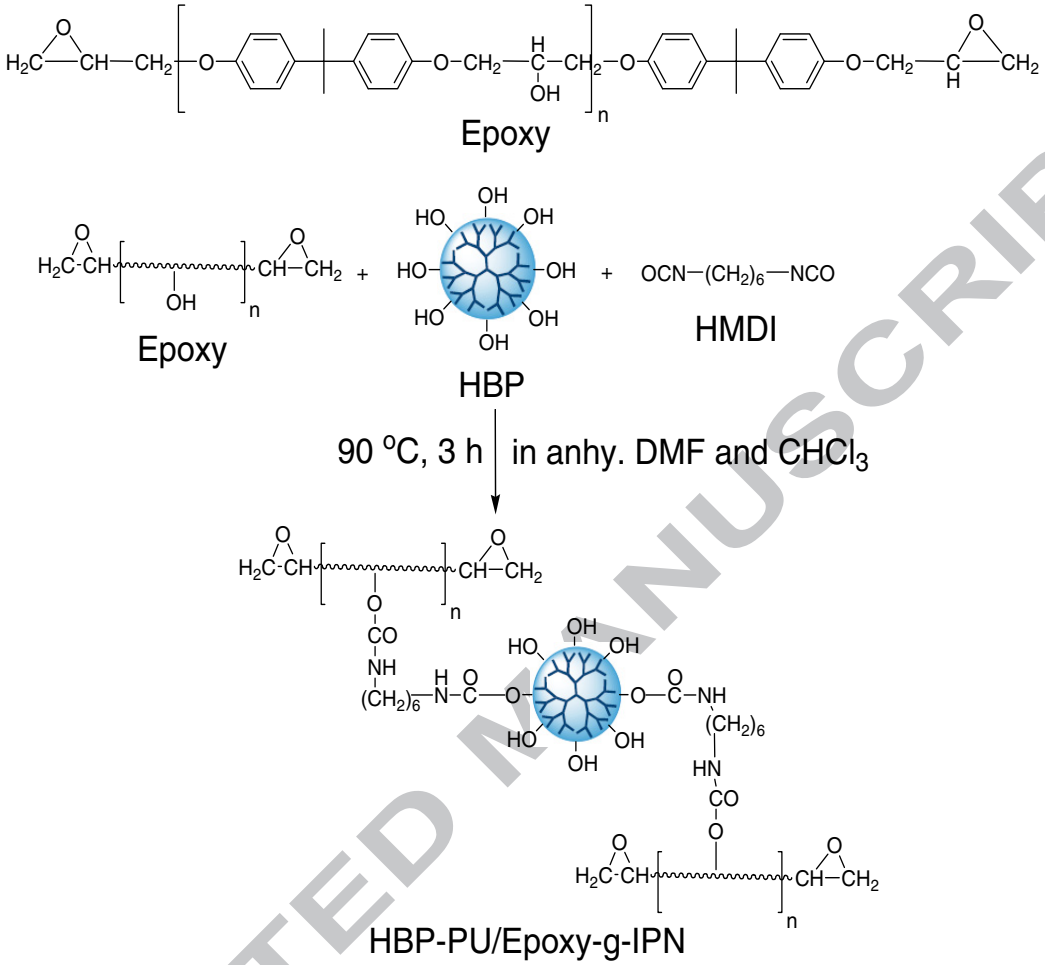

Scheme 5 Reaction pathway for the formation of HBP-PU/Epoxy-g-IPN.

2.4. Spectral characterization

Fourier transform infrared (FTIR) spectra were recorded using Bruker 66V FT-IR spectrophotometer at a resolution of 4 cm^{-1} with 32 scans. ^{1}H and ^{13}C NMR spectra were recorded using Ascend^{TM} (Brucker, Germany) 400-MHz spectrometer in hexadeuterated dimethyl sulfoxide (DMSO-d6) with trimethylsilane as an internal standard. Sample for MALDI-TOF MS analysis was prepared by dissolving each HBP sample in DMF solvent using α-cyano-4-hydroxycinnamic acid as the matrix. The resulting mixture was spotted onto a freshly cleaned stain less steel MALDI target plate. After air drying, the crystallized spots were processed using Voyager DE PRO Biospectrometry Workstation (USA). MS was recorded in a linear mode. A pulsed nitrogen laser of 337 nm was used (maximum firing rate: 20 Hz, maximum pulse energy:

300 µJ) for desorption-ionization and TOF was operated in a delayed extraction mode. Ions were accelerated into the analyzer at a voltage of 25 kV. The mass spectra were collected in both the negative and positive ion modes at an average of 100 shots.

2.5. Intrinsic viscosity measurement

Viscosity measurements of synthetic polymer solutions can be used to deduce the degree of branching, the shape and volume of the macromolecule itself. In our study, the initial polymer solution (5.025 g) was prepared by dissolving in 100 ml of NMP solvent and kept stirring overnight. The efflux time for the NMP solvent (t_s) was measured using Ubbelohde viscometer (AVS 260 Schott–Gerate GmbH) immersed in a water bath thermostated at 25 ^{o}C. The stirred polymer solution was filtered using a 25 µm PTFE filter, and 20 ml of this polymer solution was transferred to the viscometer. After measuring the efflux time for initial polymer concentration, the apparatus automatically makes four more dilutions by taking neat solvent from the reservoir using a differential pressure. Efflux time for each concentration was calculated from an average of five measurements, and for a particular dilution, the flow times agreed within 0.1 s. Intrinsic viscosity [η] was determined as the common intercept of the Huggins and Kramer relationships [Eqns. (1) and (2), respectively] using [η_{sp}] and [η_r] values. The concentration of solute, c is expressed in g/dL. Eqns. (1) and (2) are fitted from the minimum squared method and the mean value of the intercepts is taken as the intrinsic viscosity [27].

$$\frac{\eta_{sp}}{c} = [\eta] + k_H[\eta]^2 c \qquad (1)$$

$$\frac{\ln \eta_r}{c} = [\eta] + k_H[\eta]^2 c \qquad (2)$$

Similarly, for HBP-G2 (4.028 g in 100 ml NMP), HBP-G3 (5.0466 g in 100 ml NMP), and HBP-G4 (5.0488 g in 100 ml NMP), the aforementioned procedure was carried out for finding the intrinsic viscosity of HBPs.

2.6. Thermal, mechanical and morphology measurements

Thermal stability was measured using SDT Q600 (Korea) by thermogravimetric analyzer (TGA) upto 600 ^{o}C (10 ^{o}C/min) under nitrogen (100 ml/min) atmosphere. Glass transition temperature (T_g) was measured using Mettler-Toledo differential scanning calorimeter (DSC) in the temperature range between -50 ^{o}C and 280 ^{o}C (10 ^{o}C/min) under nitrogen atmosphere (50

ml/min). Izod impact strength of notched epoxy and the modified epoxy samples were measured using Tinius Olsen impact tester as per ASTM 256 standard. Flexural properties were measured an Instron universal testing machine (model 3382) with three-point bending mode at a cross head speed of 2 mm/min (ASTM 790). The dimensions of the samples used for mechanical studies were 80 x 10 x 4 mm, and an average of five specimens was taken for each set. Morphology of the impact test samples was observed using Scanning Electron Microscopy (SEM, Hitachi S-3400N) with the magnification ranging from 20 to 3,00,000x.

3. Results and Discussion

3.1. Spectral analysis of HBPs

Fig. 1 shows the FTIR spectra of the synthesized HBPs as a function of varying generations (HBP-G1 to HBP-G4). The broad band at 3200-3600 cm^{-1} corresponds to the presence of hydrogen bonded hydroxyl group. The peaks at 2941 and 2884 cm^{-1} correspond to the CH_3 and CH_2 stretching vibrations whereas the CH_2 and CH_3 bending deformation vibrations appear at 1472 and 1375 cm^{-1}, respectively. The medium band at 1400 cm^{-1} indicates the existence of -OH in-plane bending, while the very weak band at 764 cm^{-1} denotes the presence of -OH out-of-plane bending. The strong bands at 1223 and 1128 cm^{-1} represent the C-O-C=O stretching of ester and C-O-C=O stretching of ester groups, respectively. The C-O stretching of -CH_2OH groups is detected from the band at 1043 cm^{-1}. Interestingly, the ester carbonyl group exhibit a small but significant shift towards higher wave number as observed from the bands at 1729 cm^{-1} (HBP-G1), 1733 cm^{-1} (HBP-G2), 1734 cm^{-1} (HBP-G3) and 1734 cm^{-1} (HBP-G4), which clearly indicates a decrease in the extent of H-bonding between carbonyl and hydroxyl groups with increasing generations.

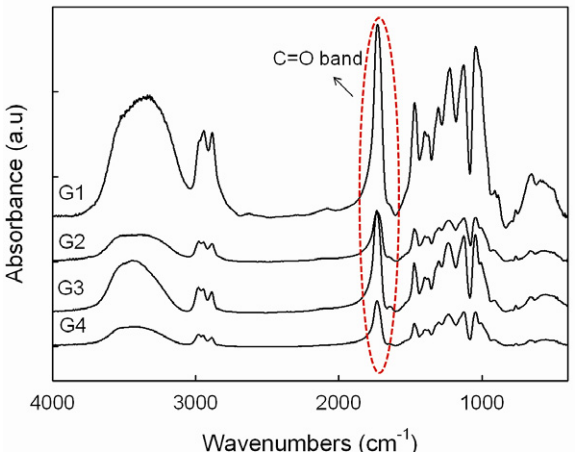

Fig. 1. FTIR spectra of HBPs as a function of varying generations (G1-G4).

The representative NMR spectra of HBP-G3 and HBP-G4 are shown in Figs. 2 and 3. The ^{1}H NMR spectra [Fig. 2(a) and 3(a)] clearly show the resonance signals of $-CH_3$ group appearing at around 0.7-0-1.1 ppm, whereas $-CH_2$ groups attached to reacted hydroxyl groups (CH_2-O-C=O) and unreacted hydroxyl groups (CH_2-OH) resonate at around 4.1-4.0 and 3.4 ppm, respectively, regardless of the HBP generations. The terminal and linear hydroxyl ($-OH_T$ and $-OH_L$) groups appear at around 4.6 and 5.0 ppm, respectively. The ^{13}C NMR spectra of HBP-G3 and HBP-G4 depicted in Figs. 2(b) and 3(b) respectively show the appearance of methyl carbons in the range of 16-18 ppm, whereas quaternary carbons appear in the region between 45 and 51 ppm. Methylene carbons and carbonyl carbons of the HBPs can be detected from the peaks observed in the range of 62-68 ppm and 170-175 ppm, respectively. The peaks at around 49.4 and 47.5 ppm correspond to terminal acid (T_{acid}) and linear acid (L_{acid}) units. Absence of any side reaction (etherification) during the synthesis of hyperbranched polyester could be confirmed from the absence of peaks at 49.3 and 47.3 ppm in the quaternary carbon region corresponding to linear ether (L_{ether}) and dendritic ether (D_{ether}) units, respectively. Further confirmation for the absence of etherification reaction could be corroborated from the non-existent peak at around 72-75 ppm in the methylene region [28]. The presence of terminal (T), linear (L), and dendritic (D) repeating units of quaternary carbon are observed from the peaks at around 50.2, 48.2 and 46.2 ppm, respectively while in the carbonyl carbon region, they are present at 174.3, 172.9 and 171.8 ppm for T, L, and D, respectively. The signal at 176.6 ppm confirms the presence of –COOH group in HBPs. The structural units found in the HBPs are shown in the Scheme 6.

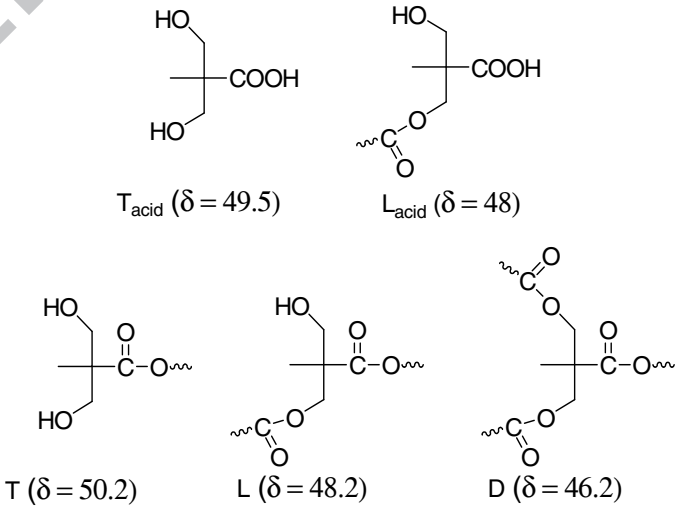

Scheme 6 Structural units found in the HBPs (HBP-G1 to HBP-G4).

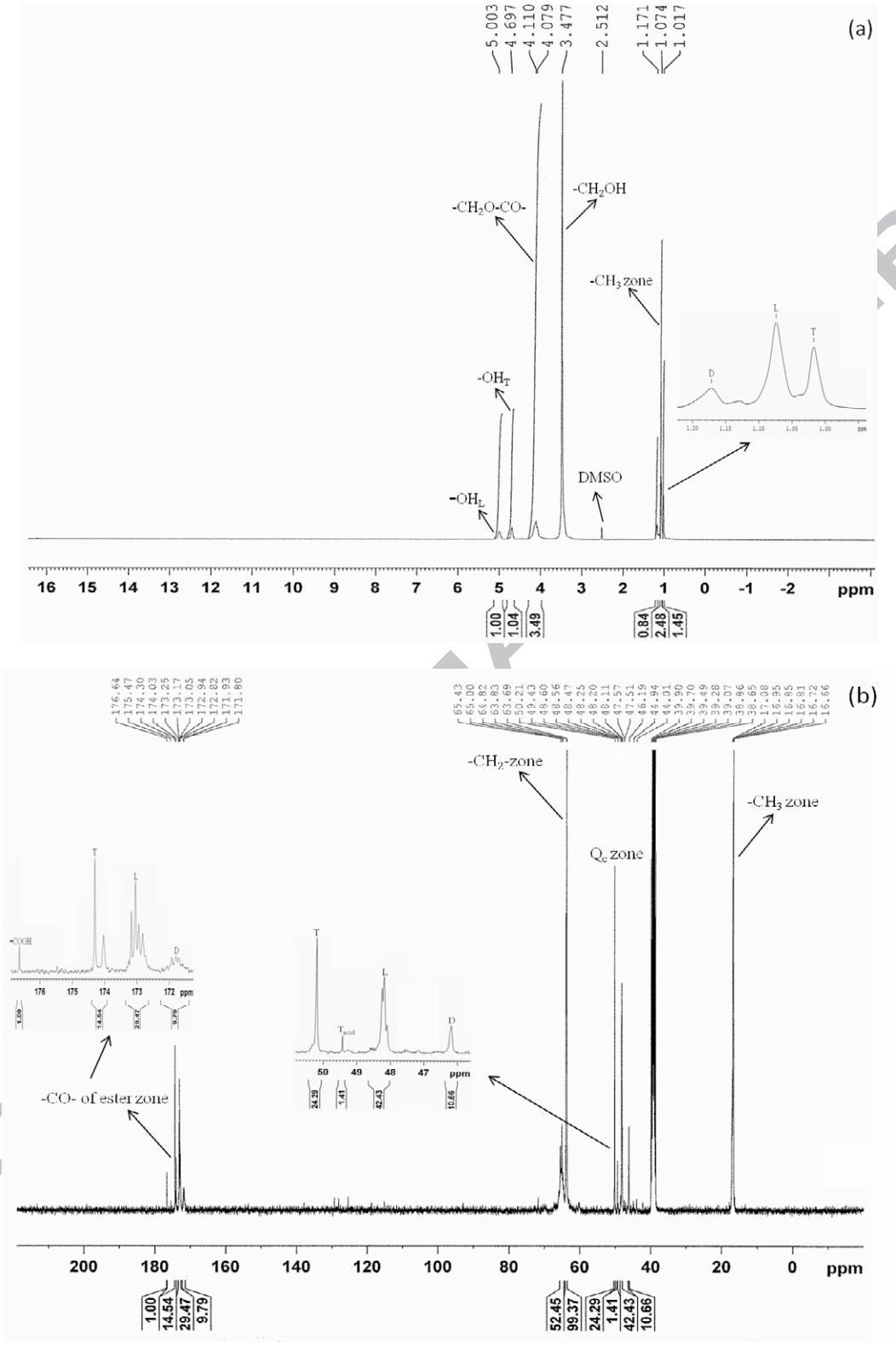

Fig. 2. (a) ^{1}H NMR and (b) ^{13}C NMR spectra of HBP-G3.

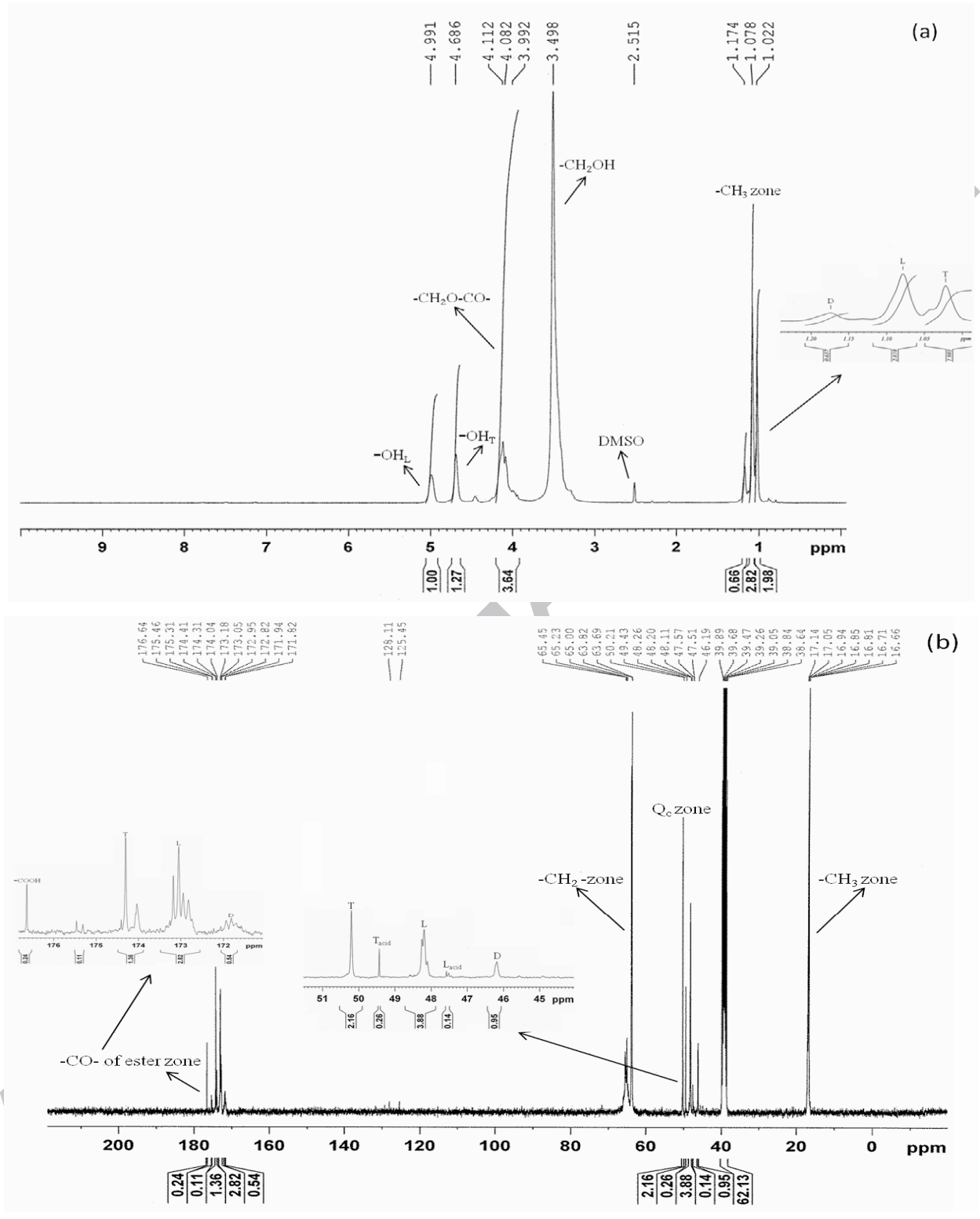

Fig. 3. (a) ^{1}H NMR and (b) ^{13}C NMR spectra of HBP-G4.

Table 3 shows the degree of branching by Frechet and Frey method [29, 30] calculated using Eqns. (3) and (4), and the data indicate that the polymer formed is highly branched.

$$DB_{Frechet} = \frac{D+T}{D+L+T} \quad (3)$$

$$DB_{Frey} = \frac{2D}{2D+L} \quad (4)$$

Table 3

Degree of branching of HBPs (HBP-G1 to HBP-G4).

HBPs	^{1}H-NMR		^{13}C-NMR			
	methyl zone		quaternary carbon zone		carbonyl carbon zone	
	$DB_{Frechet}$	DB_{Frey}	$DB_{Frechet}$	DB_{Frey}	$DB_{Frechet}$	DB_{Frey}
HBP-G1	0.61	0.36	0.61	0.23	0.59	0.27
HBP-G2	0.48	0.36	0.48	0.27	0.41	0.20
HBP-G3	0.48	0.40	0.45	0.33	0.45	0.40
HBP-G4	0.48	0.32	0.44	0.33	0.40	0.28

3.2. Thermal and physical properties of HBPs

Fig. 4 presents the thermal stability of HBPs studied using TGA measurement. An in-depth analysis reveals the measurable weight loss to occur between 230 and 275 ^{o}C for all the samples. Below 230 ^{o}C, there is no measurable amount of evaporable compounds such as moisture and unreacted monomers. The onset of thermal degradation for HBP-G1 and HBP-G2 was found to be at 314 ^{o}C whereas for HBP-G3 and HBP-G4, the weight loss starts occurring at near 325 ^{o}C. This clearly indicates that the thermal stability of HBP increases with increasing generations due to enhancement in the backbone structure as well as raised number of end functional groups. The temperature at which weight loss of 5, 20, 50, and 80 % (designated as T_5, T_{20}, T_{50}, and T_{80}) occurs was observed to increase with increasing generations as shown in Table 4. The increase in thermal stability is more prominent with increasing generation from first to second but reaches a plateau at higher generations. Overall, the increasing in degradation temperature with increasing HBP generations is attributed to an increase in molar mass along with an increase in the number of hydroxyl end groups per macromolecules and the formation of intramolecular hydrogen bridges between –OH groups in the same branches.

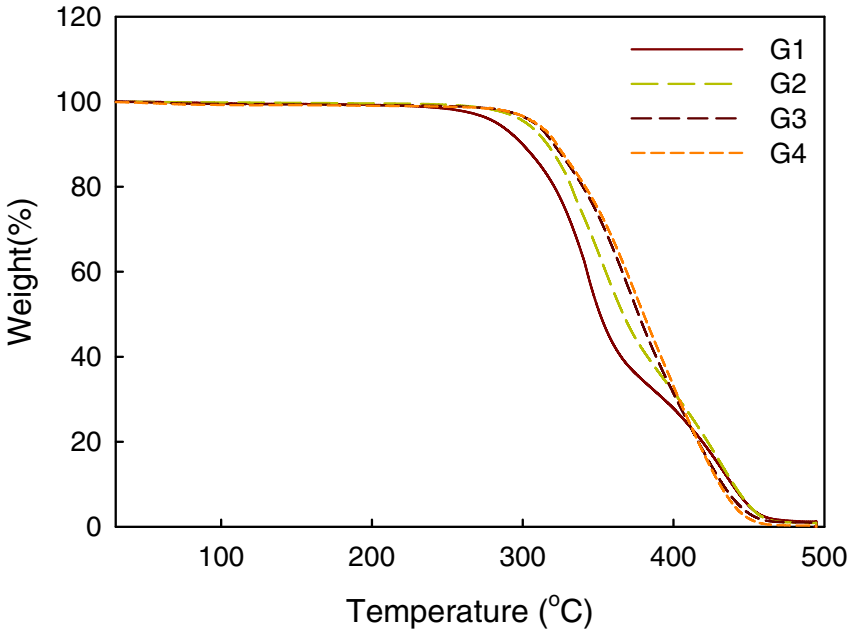

Fig. 4. TGA curves of HBPs (HBP-G1 to HBP-G4).

Table 4

Degradation temperatures of different HBP generations (G1-G4).

HBPs	T_5 (°C)	T_{20} (°C)	T_{50} (°C)	T_{80} (°C)
HBP-G1	283	321	351	419
HBP-G2	303	333	367	423
HBP-G3	308	340	377	417
HBP-G4	310	342	380	417

Thermal properties of hyperbranched polymers are significantly different from those of linear analogous of same nature and molar mass. Being amorphous in nature, the highly branched structure of hyperbranched polymer significantly affects the T_g. Fig. 5 shows the DSC curves as a function of varying HBP generations. The glass transition temperature (T_g) is enhanced with increasing number of generations due to the growth in branching which restricts the mobility of the backbone. However, a slight decrease in the T_g for HBP-G4 than that of HBP-G3 may be attributed to an increase in free volume by the end groups and reduction of the extent of H-bonding by the end groups [31]. The second order transition exhibited by HBPs in the

present study is mainly due to the translational motion of the molecule which strongly depends on the molecular mobility of the back bone rather than the segmental chain motion, and also on the type and number of the end functional groups, number of crosslinks or branching points to some extent and more polarity of the end groups [32-34].

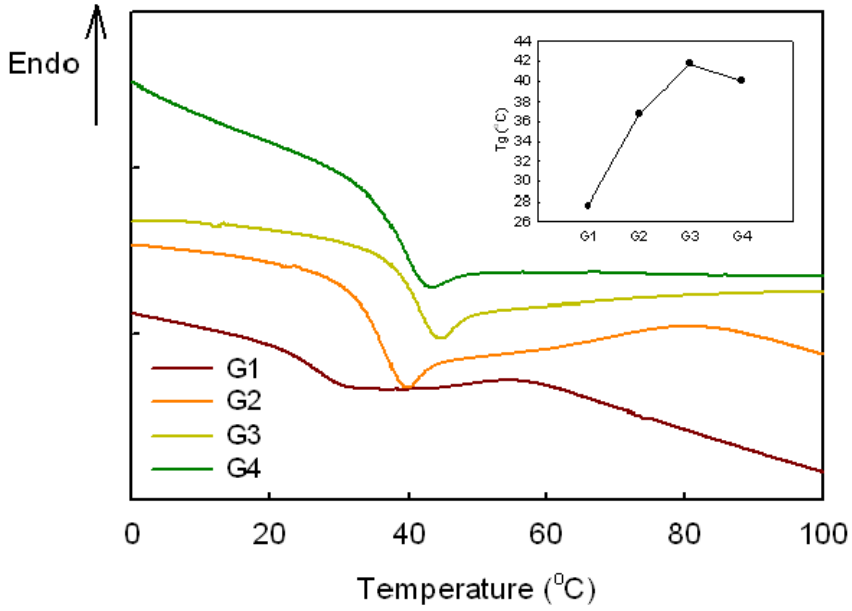

Fig. 5. Second order transition from DSC curves of different generations of HBPs (G1 to G4).

Table 5 presents the inherent viscosity, polydispersity index (PDI), number average (M_n) and weight average (M_w) molecular weight of the synthesized HBPs. Lower inherent viscosity value indicate that HBPs are in globular shape, which increases slightly with increase in molar mass or with different generations. PDI data indicate that the HBPs are heterogeneous.

Table 5

Inherent Viscosity and MALDI-TOF data of different HBP generations (G1-G4).

HBPs	Inherent Viscosity [η] (dL/g)	M_n (g/mol)	M_w (g/mol)	PDI = M_w/M_n
HBP-G1	0.0690	525	737	1.40
HBP-G2	0.0773	1586	2138	1.35
HBP-G3	0.0915	5330	5469	1.03
HBP-G4	0.1042	-	-	-

3.3. Mechanical properties of HBP-PU/Epoxy-g-IPNs

As discussed in the experimental part, the synthesized HBPs were reacted with epoxy resin through the formation of PU linkages. The IPNs were analyzed for their mechanical properties as a function of varying HBP generations. Fig. 6(a) shows the impact strength of epoxy and the modified epoxy samples. Except L-PU/EP sample (used for comparison), all the HBP modified epoxy samples (represented as G1, G2, G3 and G4) exhibit higher impact resistance compared to that of neat epoxy. Though the impact strength decreased for G4 compared to G3, it is still higher than that of neat epoxy by 6 %. Among the modified samples, the maximum impact strength exhibited by G3 sample (35 J/m, 9.5 % higher than neat epoxy) is attributed to the existence of well-dispersed and flexible PU linkages in the epoxy matrix leading to more ductility of the matrix. The decrease in impact strength for G4 sample is due to the formation of bigger size of rubber particles as confirmed from the SEM image [Fig. 8(g)]. The drop in impact strength for L-PU/EP sample when compared to that of neat epoxy sample is attributed to the dominance of the macro-separated phase or aggregation of rubber particles rather than the heterogeneous morphology in the matrix as proved by the SEM image [Fig. 8(b)]. Fig. 6(b) depicts the flexural strength and modulus of neat epoxy and modified epoxy samples. Overall, the modified samples (G1 to G4) exhibit lower flexural characteristics than that of neat epoxy as well as L-PU/EP sample owing to the incorporation of rubber particles into the epoxy matrix leading to its flexibility. However, among G1 to G4, the flexural strength and modulus increased linearly with increasing generation number due to increase in rigidity of the materials.

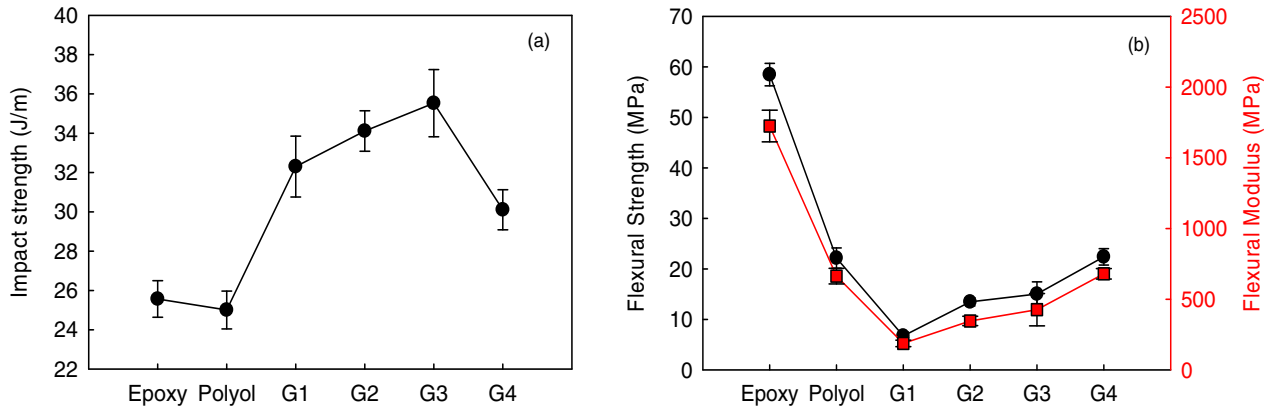

Fig. 6. (a) Izod impact strength and (b) Flexural properties of Epoxy and the modified PU/epoxy-g-IPNs of different generations (G1 to G4) of HBP and linear polyol sample.

3.4. Thermal properties of HBP-PU/Epoxy-g-IPNs

The thermogravimetric curves for modified and unmodified epoxy samples are depicted in Fig. 7(a). The thermal stability of the samples decreased linearly with increasing generations of HBP owing to presence of thermally weak and flexible polyurethane linkages (NH-CO) in the modified epoxy samples. The onset temperature is found to be 339, 333, 323, 321, 318, and 316 ^{o}C for epoxy, L-PU/EP, G1-PU/EP, G2-PU/EP, G3-PU/EP and G4-PU/EP samples, respectively. The temperatures at which weight loss of 20, 40, and 60 % (designated as T_{20}, T_{40}, and T_{60}) is represented in Table 6. Fig. 7(b) exhibits the DSC curves of epoxy and its modified samples. The modified samples exhibit lower glass transition temperature (T_g) in comparison with neat epoxy sample. The observed lowering of T_g in the modified samples when compared to neat epoxy is attributed to the existence of flexible polyurethane linkages which reduces the effective crosslink density leading to increase in the free volume for molecular relaxation.

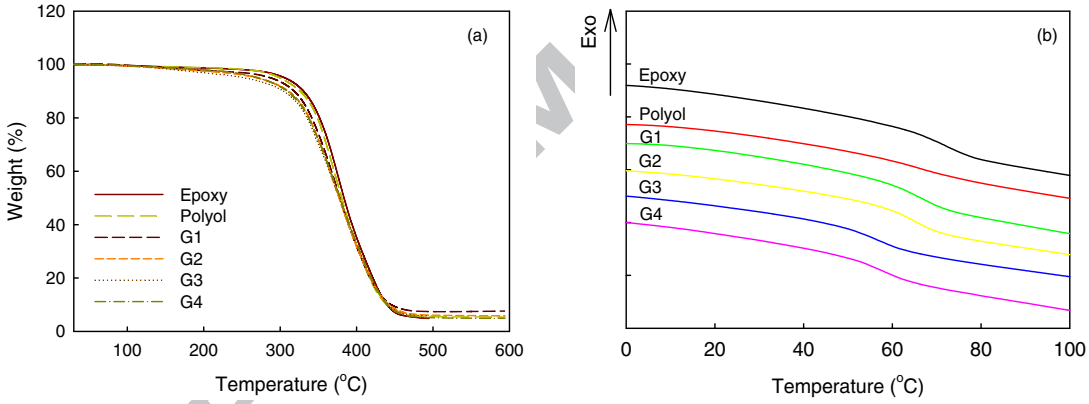

Fig. 7. (a) TGA and (b) DSC curves of epoxy and its modified samples.

Table 6

Degradation temperatures for epoxy and its modified samples (HBP-PU/Epoxy-g-IPNs).

Sample code	T_{20} (^{o}C)	T_{40} (^{o}C)	T_{60} (^{o}C)
Epoxy	351	373	393
L-PU/EP	349	371	391
G1-PU/EP	342	367	389
G2-PU/EP	338	365	389
G3-PU/EP	335	364	391
G4-PU/EP	337	366	390

3.5. SEM characterization of HBP-PU/Epoxy-g-IPNs

Fig. 8 shows the SEM images of epoxy and the modified epoxy samples. Fig. 8(a) represents the glassy fractured surface with different crack planes indicating the brittle nature of epoxy sample. The modified epoxy samples exhibit two-phase morphology similar to that reported in Ref. [35]. The distribution of rubber particles in thermoset matrix indicates that the inclusion of HBP in the epoxy improved the toughness of an otherwise brittle epoxy neat sample. The grafted IPNs formed by G1-PU/EP and G2-PU/EP samples reveal segmental crack growth which reduces the rate of crack propagation in addition to two-phase morphology. Besides heterogeneous morphology, G2-PU/EP sample exhibited rubber cavitation mechanism [36] as indicated by the arrow mark in Fig. 8(d), whereas tearing of rubber particles as well as moderate size of rubber particles in comparison to that of other modified epoxy samples is responsible for greater toughness in the case of G3-PU/EP sample [Fig. 8(e)]. The presence of large-sized rubber particles in G4-PU/EP sample reduced the impact strength to some extent in comparison to that of G3-PU/EP sample while L-PU/EP sample revealed the existence of aggregation of rubber particles leading to drop in impact strength in comparison to neat epoxy sample.

4. Conclusions

In this study, four different generations of HBPs (HBP-G1 to HBP-G4) were synthesized using DIPE as a core and DMPA as AB_2 monomer, and were characterized by spectral, thermal and physical methods. The newly synthesized HBPs were confirmed to exhibit a highly branched structure but the thermal stability decreased with increasing HBP generations. The toughening of epoxy resin was accomplished by reacting each generation of the HBP with HMDI and epoxy resin leading to the formation of HBP-PU/EP-g-IPNs. Compared to neat epoxy and linear PU/EP samples, the HBP modified epoxy samples exhibit greater toughness as observed from the higher impact strength values, which is attributed to the two-phase morphology and tearing of rubber particles which reduces the rate of crack propagation as confirmed from the SEM micrographs. Flexural, thermal stability as well as T_g properties of the modified epoxy samples are lower than that of neat epoxy sample owing to the incorporation of flexible PU linkages into the epoxy resulting in reduced crosslink density of the thermoset epoxy matrix. The data obtained from the present study will be useful for the researchers working in the development of new toughening agents for epoxy resins for structural applications.

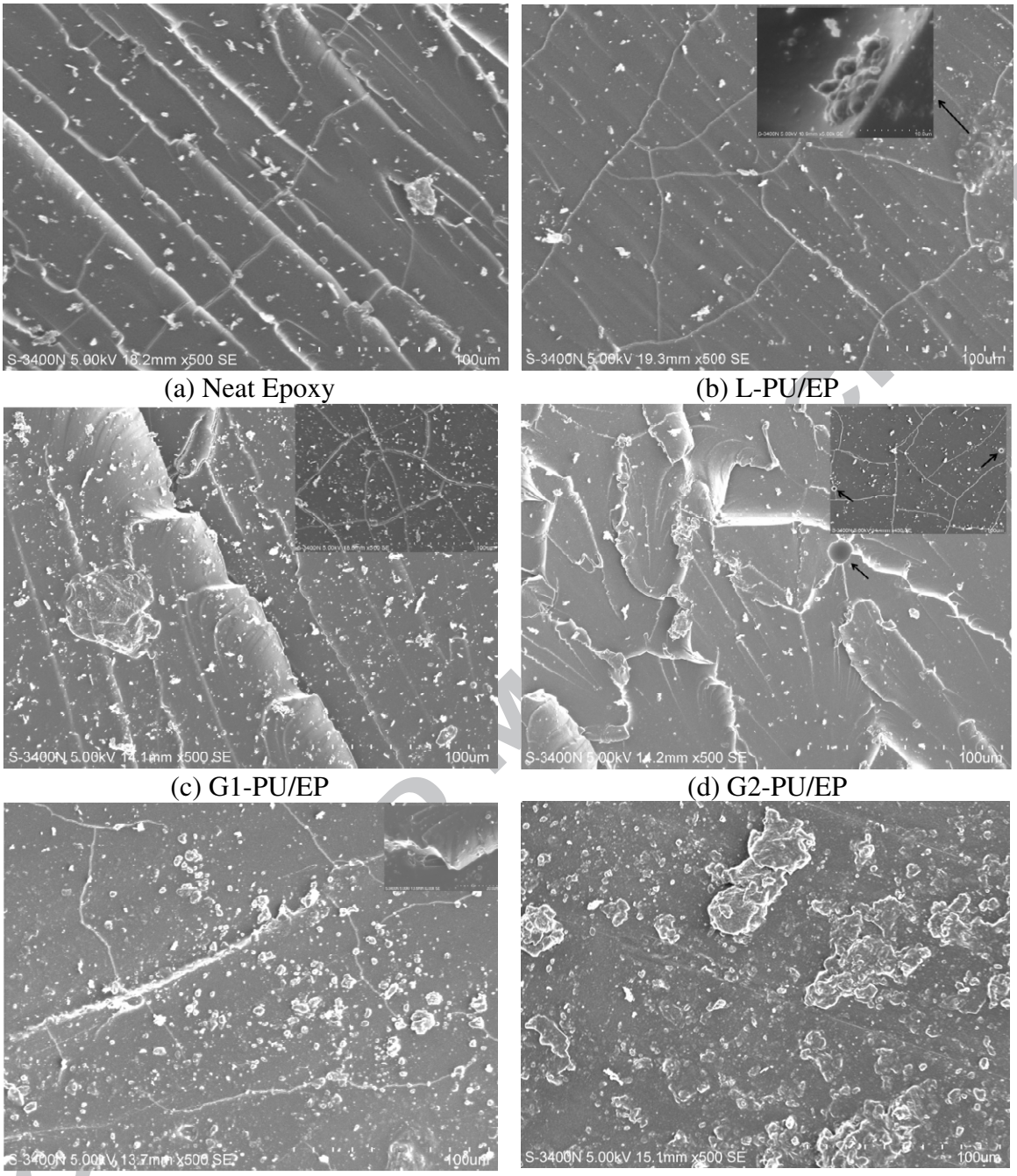

(a) Neat Epoxy (b) L-PU/EP

(c) G1-PU/EP (d) G2-PU/EP

(e) G3-PU/EP (f) G4-PU/EP

Fig. 8. SEM images of (a) Epoxy, (b) L-PU/EP, (c) G1-PU/EP, (d) G2-PU/EP, (e) G3-PU/EP and (f) G4-PU/EP samples.

Acknowledgement

The authors thank Professor A. Anand Prabu (VIT University, India) for SEM measurement and for typesetting the manuscript.

References

[1] Srivastava SK, Singh IB. Hybrid epoxy nanocomposites: Lightweight materials for structural applications. Polym J 2012; 44: 334-39.

[2] Kunz SC, Beaumont PWR. Low-temperature behavior of epoxy-rubber particulate composites. J Mater Sci 1981; 16: 3141-52.

[3] Ozturk A, Kaynak, C, Tincer T. Effects of liquid rubber modification on the behavior of epoxy resin. Eur Polym J 2001; 37: 2353-63.

[4] Abad MJ, Barral L, Cano J, López J, Nogueira P, Ramírez C, Torres A. Thermal decomposition behavior and the mechanical properties of an epoxy/cycloaliphatic amine resin with ABS. Eur Polym J 2001; 37: 1613-23.

[5] Yang K, Gu M. Fabrication, morphology and cure behavior of triethylenetetramine-grafted multiwall carbon nanotube/epoxy nanocomposites. Polym J 2009; 41: 752-63.

[6] Huang P, Zheng S, Huang J, Guo Q. Miscibility and mechanical properties of epoxy resin/polysulfone blends. Polymer 1997; 38: 5565-71.

[7] Hsieh TH, Kinloch AJ, Masania, K, Lee SJ, Taylor AC, Sprenger S. The toughness of epoxy polymers and fibre composites modified with rubber micro particles and silica nanoparticles. J Mater Sci 2010; 45: 1193-210.

[8] Hsieh KH, Han JL, Yu CT, Fu SC. Graft interpenetrating polymer networks of urethane modified bismaleimide and epoxy (I): Mechanical behavior and morphology. Polymer 2001; 42: 2491-500.

[9] Chern YC, Hsieh KH, Ma CCM, Gong YG. Interpenetrating polymer networks of polyurethane and epoxy. J Mater Sci 1994; 29: 5435-40.

[10] Prabu AA, Alagar M. Mechanical and Thermal studies of Intercross-linked networks based on siliconized polyurethane-epoxy/unsaturated polyester coatings. Prog Org Coat 2004; 49: 236-43.

[11] Prabu AA, Alagar M. Mechanical and electrical studies of silicone modified polyurethane-epoxy intercross-linked networks. Polym J 2004; 36: 848-55.

[12] Jia L-Y, Zhang C, Du Z-J, Li C-J, Li H-Q. Preparation of interpenetrating polymer networks of epoxy/polydimethylsiloxane in a common solvent of the precursors. Polym J 2007; 39: 593-97.

[13] Boogh L, Pettersson B, Manson, JAE. Dendritic hyperbranched polymers as toughenersfor epoxy resins. Polymer 1999; 40: 2249-61.

[14] Guo QP, Habrard A, Park Y, Halley PJ, Simon GP. Phase separation, porous structure, and cure kinetics in aliphatic epoxy resin containing hyperbranched polyester. J Polym Sci Part B: Polym Phys 2006; 44: 889-99.

[15] Ratna D, Varley R, Raman RKS, Simon GP. Studies on blends of epoxy-functionalized hyperbranched polymer and epoxy resin. J Mater Sci 2003; 38: 147-54.

[16] Zhang DH, Jia DM. Toughness and strength improvement of diglycidyl ether of bisphenol-A by low viscosity liquid hyperbranched epoxy resin. J Appl Polym Sci 2006; 101: 2504-11.

[17] Morell M, Erber M, Ramis X, Ferrando F, Voit B, Serr A, New epoxy thermosets modified with hyperbranched poly(ester-amide) of different molecular weight. Eur Polym J 2010; 46: 1498-09.

[18] Verrey J, Winkler Y, Michaud V, Manson J-AE. Interlaminar fracture toughness improvement in composites with hyperbranched polymer modified resin. Compos Sci Tech 2005; 65: 1527-36.

[19] Frisch HL, Frisch KC, Klempner D. Glass transitions of topologically interpenetrating polymer networks. Polym Eng Sci 1974; 14: 646-50.

[20] Wang HH, Chen JC. Modification and compatibility of epoxy resin with hydroxyl-terminated or amine-terminated polyurethanes. Polym Eng Sci 1995; 35: 1468-75.

[21] Harani H, Fellahi S, Bakar M. Toughening of epoxy resin using synthesized polyurethane prepolymer based on hydroxyl-terminated polyesters. J Appl Polym Sci 1998; 70: 2603-18.

[22] Premkumar S, Chozhan CK, Alagar M. Studies on thermal, mechanical and morphological behaviour of caprolactam blocked methylenediphenyl diisocyanate toughened bismaleimide modified epoxy matrices. Eur Polym J 2008; 44: 2599-07.

[23] Sung PH, Wu WG. Graft copolymer networks of polyurethane and epoxy structures I. Dynamic mechanical properties. Eur Polym J 1994; 30: 905-9.

[24] Chern YC, Hsieh KH, Ma CCM, Gong YG. Interpenetrating polymer networks of polyurethane and epoxy. J Mater Sci 1994; 29: 5435-40.

[25] Lin SP, Han JL, Yeh JT, Chang FC, Hsieh KH. Composites of UHMWPE fiber reinforced PU/epoxy grafted interpenetrating polymer networks, Eur Polym J 2007; 3: 996-1008.

[26] Jena KK, Raju KVSN. Synthesis and characterization of hyperbranched polyurethane-urea/silica based hybrid coatings. Ind Eng Chem Res 2007; 46: 6408-16.

[27] Bustamante P, Lupion JN, Escalera B. A new method to determine the partial solubility parameters of polymers from intrinsic viscosity. Eur J Pharma Sci 2005; 24: 229-37.

[28] Zagar E, Zigon M. Aliphatic hyperbranched polyesters based on 2,2-bis(methylol)propionic acid—Determination of structure, solution and bulk properties. Prog Polym Sci 2011; 36: 53-88.

[29] Hawker CJ, Lee R, Frechet JMC. One-step synthesis of hyperbranched dendritic polyesters. J Am Chem Soc 1991; 113: 4583-8.

[30] Hoelter D, Burgath A, Frey H. Degree of branching in hyperbranched polymers. Acta Polym 1997; 48: 30-5.

[31] Luciani A, Plummer CJG, Nguyen T, Garamszegi L, Manson JAE. Rheological and physical properties of aliphatic hyperbranched polyesters. J Polym Sci Part B: Polym Phys 2004; 42: 1218-25.

[32] Inoue K. Functional dendrimers, hyperbranched and star polymers. Prog Polym Sci 2000, 25: 453-571.

[33] Farrington PJ, Hawker CJ, Fréchet JMJ, Mackay ME. The melt viscosity of dendritic poly(benzylether) macromolecules. Macromolecules 1998; 31: 5043-50.

[34] Wooley KI, Hawker CJ, Pochan JM, Frechet JMJ. Physical properties of dendritic macromolecules: a study of glass transition temperature. Macromolecules 1993; 26: 1514-19.

[35] Mahesh KPO, Alagar M, Kumar SA. Mechanical, thermal and morphological behavior of bismaleimide modified polyurethane-epoxy IPN matrices. Polym Adv Technol 2003; 14: 137-46.

[36] Fu J-F, Shi L-Y, Yuan S, Zhong Q-D, Zhang D-S, Chen Y, Wu J. Morphology, toughness mechanism, and thermal properties of hyperbranched epoxy modified diglycidyl ether of bisphenol A (DGEBA) interpenetrating polymer networks. Polym Adv Technol 2008; 19: 1597-607.

List of Schemes

List of Figures

List of Tables

Graphical Abstract

Title:
Effect of New Hyperbranched Polyester of Varying Generations on Toughening of Epoxy Resin through Interpenetrating Polymer Networks using Urethane Linkages – D. Manjula Dhevi et al.